



Electrically evoked compound action potentials are associated with the site of intracochlear stimulation

Nora M. Weiss^{1,2,3} · Tabita Breitsprecher¹ · Christiane Völter¹ · Marc Lammers^{2,4} · Paul Van de Heyning^{2,4} · Stefan Dazert¹ · Vincent Van Rompaey^{2,4}

Received: 7 December 2023 / Accepted: 17 January 2024
© The Author(s) 2024

Abstract

Objectives Objective measurements to predict the position of a cochlear electrode during cochlear implantation surgery may serve to improve the surgical technique and postoperative speech outcome. There is evidence that electrically evoked compound action potentials (ECAP) are a suitable approach to provide information about the site of stimulation. This study aims to contribute to the knowledge about the association between the intraoperative intracochlear ECAP characteristics and the site of stimulation.

Methods In a retrospective cohort study, patients undergoing cochlear implant surgery with flexible lateral wall electrode arrays (12 stimulating channels) between 2020 and 2022 were analyzed. The CDL was measured using a CT-based clinical planning software. ECAP were measured for all electrode contacts and associated to the CDL as well as to the site of stimulation in degree.

Results Significant differences among the amplitudes and slopes for the individual stimulated electrode contacts at the stimulation sites of 90°, 180°, 270°, 360°, 450° and 540° were found. The values showed a trend for linearity among the single electrodes.

Conclusions ECAP characteristics correlate with the electrode's position inside the cochlea. In the future, ECAP may be applied to assess the intracochlear position inside the cochlea and support anatomy-based fitting.

Keywords ECAP characteristics · Electrode position · Anatomy-based fitting · Patient-individualized cochlear implantation

Introduction

Recently, objective measurement methods are increasingly becoming topics of interest in the treatment of patients with severe to profound hearing loss with a cochlear implant (CI), especially with regard to implant fitting in children

or patients with poor compliance [1–4]. Furthermore, in this context, the position of the electrode and the angle of insertion are of interest for improving the hearing perception outcome [5]. The electrically evoked compound action potentials (ECAP) are considered a promising approach for CI fitting [6, 7] especially in children, since they are able to provide objective information about the stimulation thresholds. There is evidence that ECAP are also suitable to provide information not only about the neural integrity of spiral ganglion neurons but also about the site of stimulation [8–10]. The electrode position inside the cochlear is of interest for anatomy-based fitting approaches that have been shown to provide improved speech perception [11, 12]. However, the size of the human cochlea can significantly affect the CI electrode position within the cochlea and consequently structure preservation as well as the final pitch discrimination [13, 14]. Consequently, choosing the electrode variant fitting the individual expectations is highly relevant. To predict the postoperative electrode position from

✉ Nora M. Weiss
nora.weiss@rub.de

¹ Department of Otorhinolaryngology-Head and Neck Surgery, Ruhr-University Bochum, St. Elisabeth-Hospital Bochum, Bochum, Germany

² Department of Translational Neurosciences, Faculty of Medicine and Health Sciences, University of Antwerp, Antwerp, Belgium

³ International Graduate School of Neuroscience (IGSN), Ruhr-University Bochum, Bochum, Germany

⁴ Department of Otorhinolaryngology and Head and Neck Surgery, Antwerp University Hospital, Antwerp, Belgium

preoperative clinical imaging, it has been demonstrated that a clinical planning software for measuring the human cochlea (Otoplan, Cascination, Bern, Switzerland) is adequate to determine the length of the cochlear duct and to select the electrode length according to the aimed insertion depth [15]. However, it has been shown that there are inaccuracies concerning the insertion depth prediction of the software [16]. Thus, a feedback mechanism providing intraoperative information about the insertion depth is desirable. Thus, the aim of this work was to determine reference values for ECAP characteristics at different locations inside the cochlea. This study aims to contribute to the knowledge about the association between changing ECAP characteristics inside the cochlea according to the CDL.

Methods

Patients selection

Between 2020 and 2022, patients scheduled for cochlear implant surgery due to severe and profound hearing loss were assessed for inclusion. Patients implanted with flexible lateral wall electrode arrays with 12 stimulating channels (Med-el GmbH, Innsbruck, Austria) without functional residual hearing were included into the study. Patients with insufficient imaging quality to identify the postoperative electrode position were excluded. The study protocol was approved by the local Ethics Committees in accordance with the Helsinki declaration.

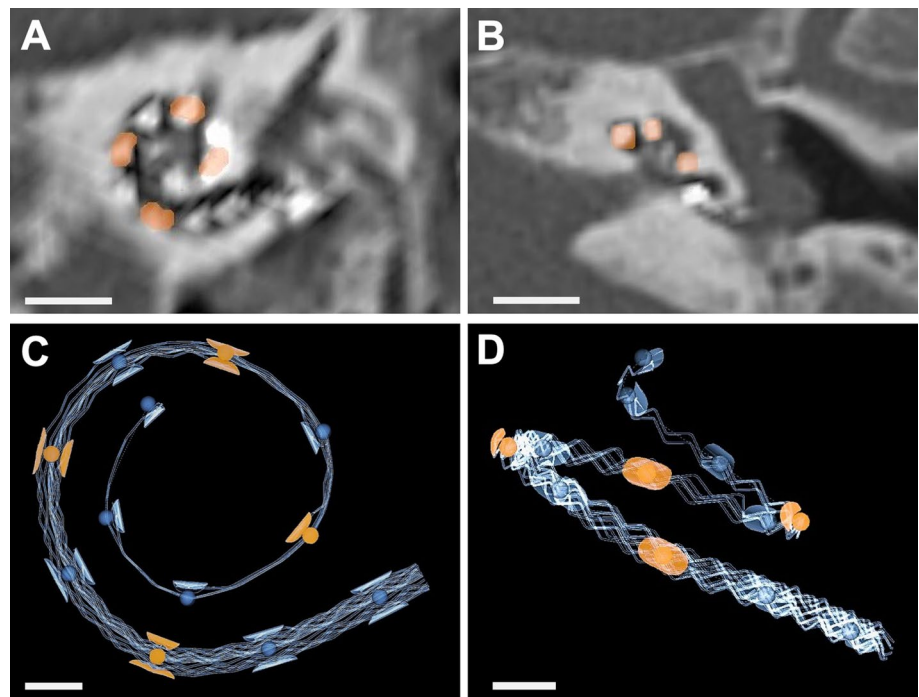
Preoperative determination of cochlear duct length and estimation of cochlear coverage

All measurements were performed using an otosurgical planning software (Otoplan, Cascination AG, Bern, Switzerland). The pre-defined anatomical landmarks (the round window and lateral wall of the cochlea) to determine the diameter (*A* value) and the width (*B* value: perpendicular to the line segment of the *A* value, intersecting the *A* value line at the modiolus) of the cochlea were marked by a single investigator experienced in the interpretation of temporal bone imaging. The calculation of the CDL approximation is performed by the software based on an elliptic circular approximation [29]. The electrode length was chosen to cover 75% of the CDL according to the preoperative CDL estimation.

Postoperative determination of insertion angle and cochlear coverage

The postoperative insertion angle was measured on postoperative high resolution computed tomography (HRCT) imaging control. The round window was localized, and the individual electrode contacts were marked manually (Fig. 1A). The software output is the insertion angle in degree. In addition, the individual electrode contact positioned at 90°, 180°, 270°, 360°, 450° and 540° were determined manually (Fig. 1B).

Fig. 1 Postoperative angular insertion depth determination. **A** Postsurgical CT-scan oblique coronal view. Electrode array positioned along the lateral cochlear wall. Electrode contacts entering the cochlea 90°, 180°, 270° and 360° are marked in orange. **B** Postsurgical CT-scan axial view. Scale bar 5 mm. **C** Three-dimensional electrode array reconstruction from oblique coronal view. Electrode contacts entering the cochlea 90°, 180°, 270° and 360° are marked in orange. **D** Three-dimensional electrode array reconstruction from axial view. Scale bar 1 mm



ECAP measurements

ECAP measurements were performed using the Med-el fitting software (Maestro version 6.0.1, 7.0.1 and 8.0.1, Med-el GmbH, Innsbruck, Austria). The ECAP stimulation of every individual electrode was recorded. The electrode located apical to the stimulating electrode was used as the recording electrode. When electrode 1 (most apical) was stimulated, electrode 2 (more basal electrode) was used as the recording electrode. The stimulation protocol was chosen as follows: inter phase gap $2.10\text{E}-06$ s; maximum charge: 35 qu, phase duration $4.00\text{E}-05$ s. The stimulation charge was increased up to 50 qu when no threshold was detected. For reason of homogeneity, we only used stimulation charges of 35 qu for the sub-analysis of the different insertion angles in degrees.

Statistical analysis

ECAP amplitude was defined as the voltage difference between the negative N1 peak and the following positive P2 peak. Slope of the ECAP amplitude growth function was calculated at the 50% level. Statistical analyses were performed using Prism (version 8, GraphPad Software, La Jolla, CA, USA). The significance level was set to $p < 0.05$. The assumption of normality was tested graphically using quantile–quantile plots. If not otherwise specified, data are presented as mean with standard deviation (SD) or absolute numbers with percentages. Correlations were assessed using Spearman's correlation coefficient. For comparison of > 2 groups, a one-way ANOVA was performed.

Results

A total of 64 ears from 64 CI users (mean age: 64.5 years, SD 7.8 years) were included in the present study. The patients' demographics are shown in Table 1. The electrode was inserted by round window approach in every case. The

Table 1 Patients' demographics

	Patients ($n=64$)
Mean age—years (SD)	64.5 (SD 7.8)
Sex, female:male— n (%)	28 (43.8); 36 (56.2)
Side, right:left— n (%)	31 ((48.4); 33 (51.6)
Cochlear duct length (mm)	43.7 (2.8)
Cochlear coverage (%)	65.1 (2.8)
Insertion angle (°)	585.7 (73.4)
Electrode length— n (%)	
31.5 mm	38 (59.4)
28.0 mm	22 (34.4)
26.0 mm	4 (6.2)

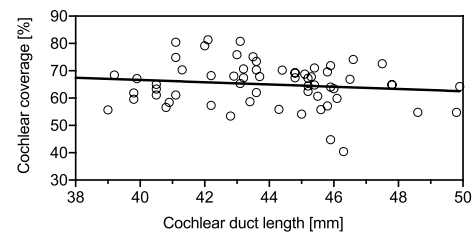


Fig. 2 Correlation of cochlear coverage (%) and cochlear duct length. Solid line represents linear regression line. r , Spearman's rank correlation coefficient

round window niche was accessed by mastoidectomy and posterior tympanotomy. Implantation and full insertion of the flexible lateral wall electrode array was achieved in all cases as verified by intraoperative impedance and ECAP measurements as well as by postoperative CT imaging. The mean cochlear duct length was 43.7 mm (SD: 2.8 mm). Mean cochlear coverage (CC) of the electrode array was 65.1% (SD 8.2%) of the CDL (Fig. 2), which corresponds to an average insertion angle of 586 degrees (SD: 73). In 36 out of 64 subjects ECAPs could be measured with a maximum stimulation charge of 35qu, in 45 patients ECAPs were measured with a maximum charge of 50qu.

ECAP measurements

There was a significant effect of electrode location on ECAP threshold, with lower thresholds at the more apical electrodes ($F(11, 367) = 4.675$, $p < 0.0001$; Fig. 3A). ECAP amplitudes were larger towards the apical end of the electrode array ($F(11, 524) = 2.083$, $p = 0.02$; Fig. 3B). The slope of the ECAP amplitude growth function, measured at the 50% level of the growth function also increased towards the apical end of the electrode array ($F(11, 362) = 9.729$, $p < 0.0001$; Fig. 3C). The effect was identical when only the subjects were included in whom ECAPs were measured up to a maximum charge of 35qu (Fig. 3D–F).

Postoperative CT reconstructions of the electrode arrays, revealed an insertion angle of 90° to correspond with electrode 9–12 (range: 3, mean: 10.20, SD: 0.78), 180° with electrode 6–10 (range 4, mean: 7.89, SD: 1.01), 270° with electrode 3–8 (range 5, mean: 5.70, SD: 1.03), 360° with electrode 1–6 (range 5, mean: 4.00, SD: 1.04), 450° with electrode 1–5 (range 4, mean: 3.05, SD: 0.94), 540° with electrode 1–4 (range 3, mean: 2.02, SD: 0.91). Figure 4 shows the increase in ECAP amplitude ($F(5, 171) = 3.164$, $p = 0.009$; Fig. 4A) and slope ($F(5, 104) = 4.188$, $p < 0.0001$; Fig. 4B) with increasing insertion angle. Simple linear regression between the insertion angles at 90° , 180° , 270° , 360° , 450° and 540° showed a significant linearity between these insertion angles and the ECAP slopes ($r = 0.98$, $p < 0.001$) as well as the ECAP amplitudes ($r = 0.95$, $p = 0.004$, Fig. 5).

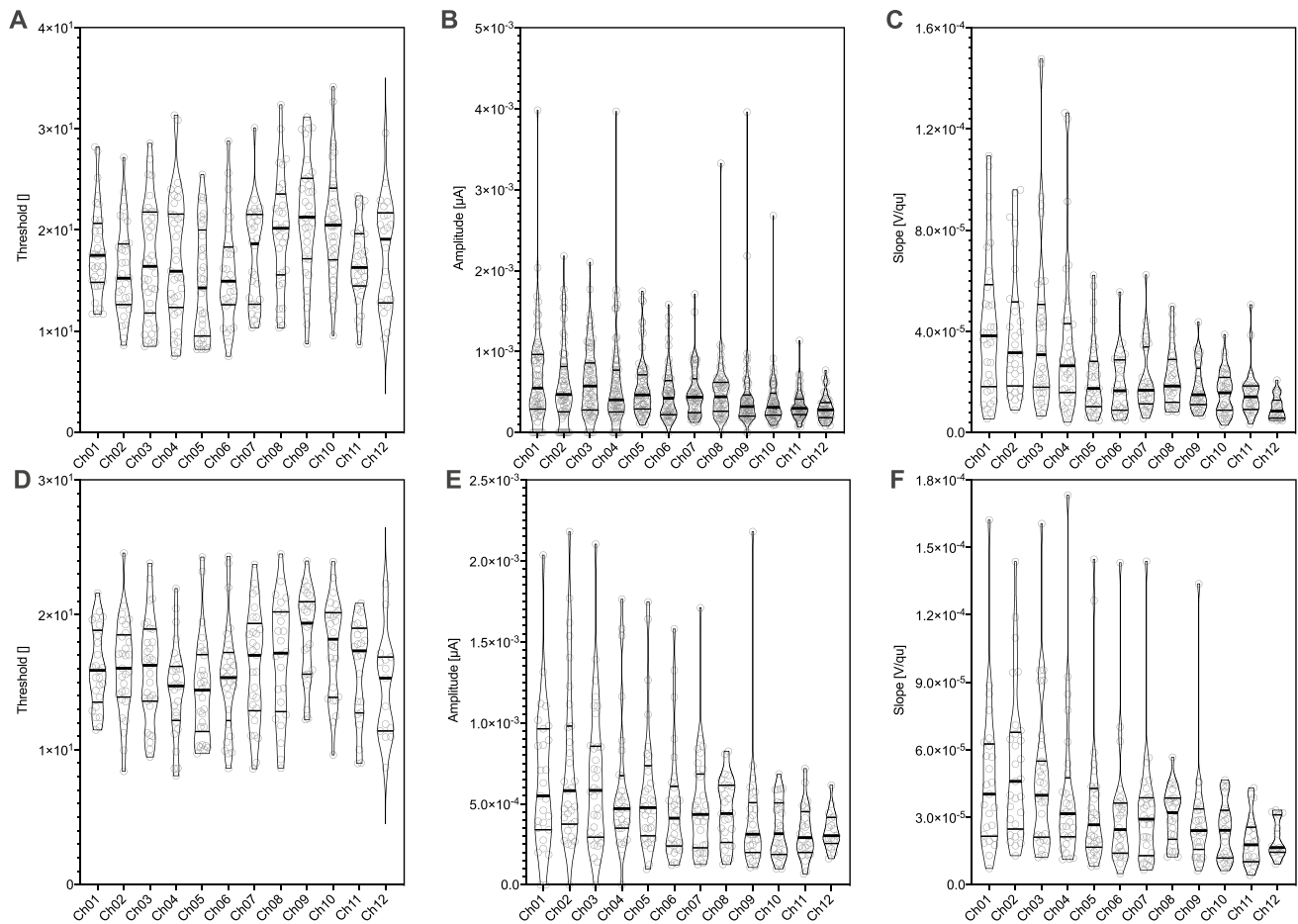


Fig. 3 ECAP characteristics and site of stimulation. **A–C** Violin plot of ECAP measured with a maximum stimulation rate of 50 qu. **A** Violin plot of ECAP threshold **B** Violin plot of ECAP amplitude and **C** Violin plot of ECAP slope for each individual stimulated electrode. **D–F** Violin plot of ECAP measured with a maximum stimulation rate of 35 qu. **D** Violin plot of ECAP threshold **E** Violin plot of ECAP

amplitude and **F** Violin plot of ECAP slope for each individual stimulated electrode. The “violin” covers the entire range of the datasets with the width indicating frequency, in analogy to a vertical diagram. Bold horizontal line indicates median, soft horizontal lines indicate interquartile ranges

Discussion

In the present study, we found a correlation between ECAP characteristics, i.e. threshold, amplitude and slope, and the site of stimulation inside the human cochlea. This is in line with a number of studies reporting variances in ECAP characteristics throughout the cochlea [9, 17–19]. A recent study reported significantly higher ECAP amplitudes throughout the apical and middle regions of the cochlea and significantly lower ECAP thresholds in patients with preserved low-frequency acoustic hearing [2]. Other explanations influencing ECAP characteristics are (1) the decreasing diameter of the cochlear turns towards the apex reducing the distance between the electrode and the neural tissue [20] and (2) an increasing density of neurons in the apical regions [21]. Nevertheless, ECAP may be a promising approach to monitor the electrode’s position during insertion.

Furthermore, the choice of the electrode array length according to the CDL seems to be feasible since there was no correlation between the CDL and the CC. Consequently, when choosing the electrode array according to the CDL homogenous ECAP characteristics among different individuals are observed. However, the mean CC was underestimated by preoperative estimation which is in line with recent studies investigating the accuracy of CC prediction [16, 22].

The findings of this study contribute to optimize existing methodologies to more accurately determine the postoperative insertion angle of the electrode array, without the need of postoperative CT imaging. This has become even more important since approaches to fit the patients speech processor to the CT-based anatomical data, is reported to result in improved hearing outcomes, music appreciation and improvements in quality of life [23–26]. In addition, it might aid in future development of methods for continuous ECAP

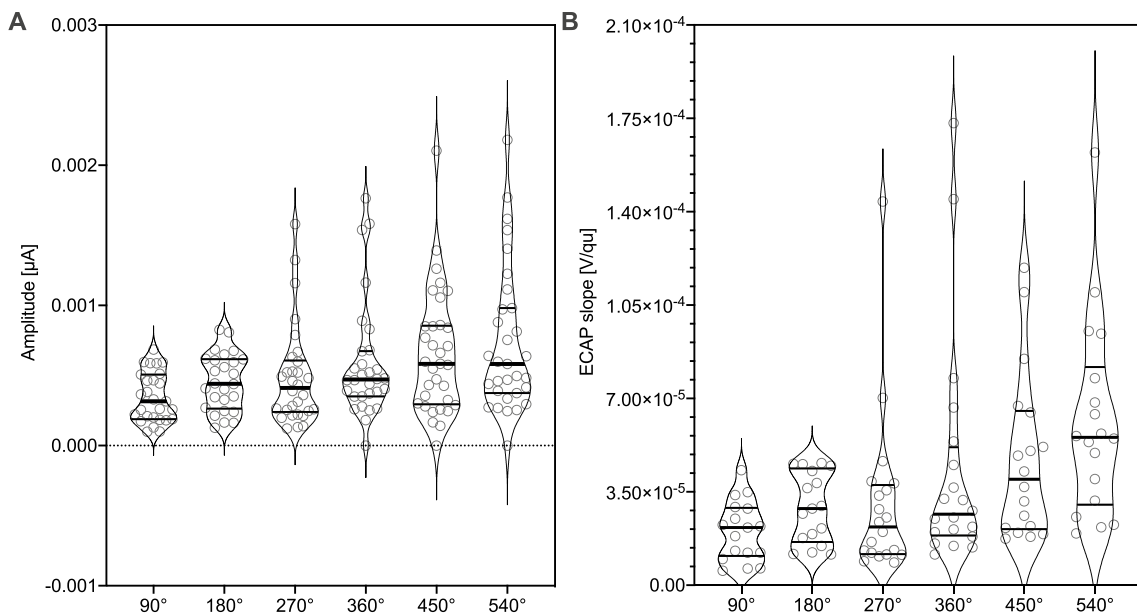
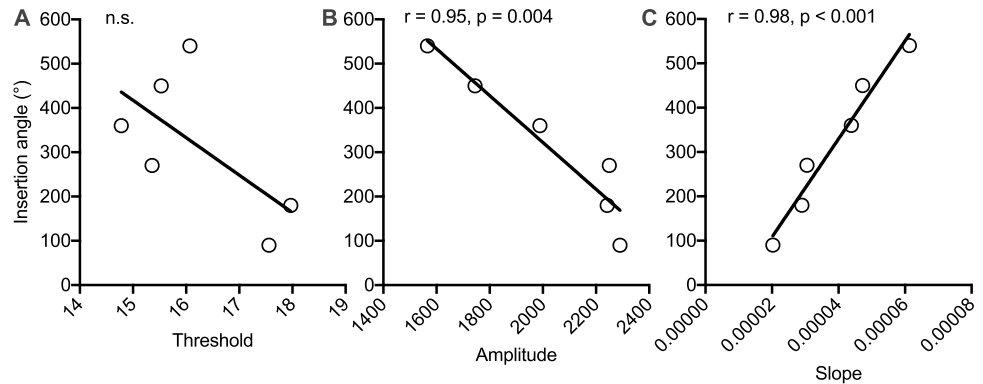


Fig. 4 ECAP characteristics and site of stimulation determined from angular electrode positioning. **A** Violin plot of ECAP amplitude and **B** violin plot of ECAP slope for the individual stimulated electrode at 90°, 180°, 270°, 360°, 450° and 540° insertion depth. The “vio-

lin” covers the entire range of the datasets with the width indicating frequency, in analogy to a vertical diagram. Bold horizontal line indicates median, soft horizontal lines indicate interquartile ranges

Fig. 5 Simple linear regression between the insertion angles at 90°, 180°, 270°, 360°, 450° and 540° and **A** ECAP thresholds, **B** ECAP amplitudes and **C** ECAP slopes. Solid line represents linear regression line. *r*, Spearman’s rank correlation coefficient



measurements to monitor and predict the intracochlear electrode array position during surgery. This can be especially relevant for cochlear implantation with the goal of electroacoustic stimulation [9] in which the position of the electrode array is adjusted to the residual hearing.

Limitations

This study is limited by heterogeneous stimulation strategies. The standard stimulation charge was set to 35 qu. However, in cases of missing thresholds, the charge was increased up to 50 qu. Consequently, comparisons among these different charges are limited. For reason of homogeneity, we only used stimulation charges of 35 qu for the sub-analysis of the

different insertion angles in degrees. However, this reduced the number of values that could be analyzed. Thus, the effect of linearity needs to be reproduced in larger cohorts.

Conclusion

ECAP characteristics are reliably associated with the electrode’s position inside the cochlea. We encourage prospective studies with standardized stimulation protocols to strengthen the results from our study under the aim of identifying standard ECAP values for the site of stimulation.

Author contributions NMW: study design, data collection, analysis, writing the manuscript. TB: radiological measurements, analysis. CV: data provision and analysis. ML, VVR, SD and PVH: scientific discussion, manuscript correction.

Funding Open Access funding enabled and organized by Projekt DEAL.

Data availability Data are available on special request when contacting the corresponding author.

Open Access This article is licensed under a Creative Commons Attribution 4.0 International License, which permits use, sharing, adaptation, distribution and reproduction in any medium or format, as long as you give appropriate credit to the original author(s) and the source, provide a link to the Creative Commons licence, and indicate if changes were made. The images or other third party material in this article are included in the article's Creative Commons licence, unless indicated otherwise in a credit line to the material. If material is not included in the article's Creative Commons licence and your intended use is not permitted by statutory regulation or exceeds the permitted use, you will need to obtain permission directly from the copyright holder. To view a copy of this licence, visit <http://creativecommons.org/licenses/by/4.0/>.

References

- Weiss BG, Sochting F, Bertlich M et al (2018) An objective method to determine the electrically evoked stapedius reflex threshold during cochlea implantation. *Otol Neurotol* 39(1):e5–e11. <https://doi.org/10.1097/MAO.0000000000001611>
- Nassiri AM, Yawn RJ, Gifford RH et al (2019) Intraoperative electrically evoked compound action potential (ECAP) measurements in traditional and hearing preservation cochlear implantation. *J Am Acad Audiol* 30(10):918–926. <https://doi.org/10.3766/jaaa.18052>
- Karatas E, Aud MD, Baglam T, Durucu C, Baysal E, Kanlikama M (2011) Intraoperative electrically evoked stapedius reflex thresholds in children undergone cochlear implantation: round window and cochleostomy approaches. *Int J Pediatr Otorhinolaryngol* 75(9):1123–1126. <https://doi.org/10.1016/j.ijporl.2011.06.002>
- de Andrade KCL, Muniz LF, Menezes PL, Neto SSC, Carnauba ATL, Leal MC (2018) The value of electrically evoked stapedius reflex in determining the maximum comfort level of a cochlear implant. *J Am Acad Audiol* 29(4):292–299. <https://doi.org/10.3766/jaaa.16117>
- Berg KA, Noble JH, Dawant BM, Dwyer RT, Labadie RF, Gifford RH (2020) Speech recognition with cochlear implants as a function of the number of channels: effects of electrode placement. *J Acoust Soc Am* 147(5):3646. <https://doi.org/10.1121/10.0001316>
- Botros A, van Dijk B, Killian M (2007) AutoNR: an automated system that measures ECAP thresholds with the nucleus freedom cochlear implant via machine intelligence. *Artif Intell Med* 40(1):15–28. <https://doi.org/10.1016/j.artmed.2006.06.003>
- Botros A, Psarros C (2010) Neural response telemetry reconsidered: I. The relevance of ECAP threshold profiles and scaled profiles to cochlear implant fitting. *Ear Hear* 31(3):367–379. <https://doi.org/10.1097/AUD.0b013e3181c9fd86>
- Jahn KN, Arenberg JG (2020) Identifying cochlear implant channels with relatively poor electrode-neuron interfaces using the electrically evoked compound action potential. *Ear Hear* 41(4):961–973. <https://doi.org/10.1097/AUD.00000000000000844>
- Mlynski R, Lüsebrink A, Oberhoffner T, Langner S, Weiss N (2021) Mapping cochlear duct length to electrically evoked compound action potentials in cochlear implantation. *Otol Neurotol* 42(3):e254–e260. <https://doi.org/10.1097/MAO.0000000000002957>
- McKay CM, Smale N (2017) The relation between ECAP measurements and the effect of rate on behavioral thresholds in cochlear implant users. *Hear Res* 346:62–70. <https://doi.org/10.1016/j.heares.2017.02.009>
- Schurzig D, Pietsch M, Erfurt P, Timm ME, Lenarz T, Kral A (2021) A cochlear scaling model for accurate anatomy evaluation and frequency allocation in cochlear implantation. *Hear Res* 403:108166. <https://doi.org/10.1016/j.heares.2020.108166>
- Kurz A, Müller-Graff F-T, Hagen R, Rak K (2022) One click is not enough: anatomy-based fitting in experienced cochlear implant users. *Otol Neurotol* 43(10):1176–1180. <https://doi.org/10.1097/MAO.0000000000003731>
- Stakhovskaya O, Sridhar D, Bonham BH, Leake PA (2007) Frequency map for the human cochlear spiral ganglion: implications for cochlear implants. *J Assoc Res Otolaryngol* 8(2):220–233. <https://doi.org/10.1007/s10162-007-0076-9>
- van der Marel KS, Briaire JJ, Wolterbeek R, Snel-Bongers J, Verbist BM, Frijns JHM (2014) Diversity in cochlear morphology and its influence on cochlear implant electrode position. *Ear Hear* 35(1):e9–20. <https://doi.org/10.1097/01.aud.0000436256.06395.63>
- Breitsprecher T, Dhanasingh A, Schulze M et al (2022) CT imaging-based approaches to cochlear duct length estimation—a human temporal bone study. *Eur Radiol* 32(2):1014–1023. <https://doi.org/10.1007/s00330-021-08189-x>
- Breitsprecher T, Mlynski R, Völter C et al (2023) Accuracy of preoperative cochlear duct length estimation and angular insertion depth. *Otol Neurotol* 44(8):e566–e571. <https://doi.org/10.1097/MAO.0000000000003956>
- Frijns JHM, Briaire JJ, de Laat JAPM, Grote JJ (2002) Initial evaluation of the Clarion CII cochlear implant: speech perception and neural response imaging. *Ear Hear* 23(3):184–197. <https://doi.org/10.1097/00003446-200206000-00003>
- Polak M, Hodges AV, King JE, Balkany TJ (2004) Further prospective findings with compound action potentials from Nucleus 24 cochlear implants. *Hear Res* 188(1–2):104–116. [https://doi.org/10.1016/S0378-5955\(03\)00309-5](https://doi.org/10.1016/S0378-5955(03)00309-5)
- Brill S, Muller J, Hagen R et al (2009) Site of cochlear stimulation and its effect on electrically evoked compound action potentials using the MED-EL standard electrode array. *Biomed Eng Online* 8:40. <https://doi.org/10.1186/1475-925X-8-40>
- Schwartz-Leyzac KC, Pfungst BE (2016) Across-site patterns of electrically evoked compound action potential amplitude-growth functions in multichannel cochlear implant recipients and the effects of the interphase gap. *Hear Res* 341:50–65. <https://doi.org/10.1016/j.heares.2016.08.002>
- Skidmore J, Ramekers D, Colesa DJ, Schwartz-Leyzac KC, Pfungst BE, He S (2022) A broadly applicable method for characterizing the slope of the electrically evoked compound action potential amplitude growth function. *Ear Hear* 43(1):150–164. <https://doi.org/10.1097/AUD.0000000000001084>
- Weiss NM, Breitsprecher T, Wozniak M, Bächinger D, Völter C, Mlynski R, Van de Heyning P, Van Rompaey V, Dazert S. Comparing linear and non-linear models to estimate the appropriate cochlear implant electrode array length—are current methods

- precise enough? *Eur Arch Otorhinolaryngol* 281(1):43–49. <https://doi.org/10.1007/s00405-023-08064-z>
23. Noble JH, Hedley-Williams AJ, Sunderhaus L et al (2016) Initial results with image-guided cochlear implant programming in children. *Otol Neurotol* 37(2):e63–e69. <https://doi.org/10.1097/MAO.0000000000000909>
 24. Jiam NT, Gilbert M, Cooke D et al (2019) Association between flat-panel computed tomographic imaging-guided place-pitch mapping and speech and pitch perception in cochlear implant users. *JAMA Otolaryngol Head Neck Surg* 145(2):109–116. <https://doi.org/10.1001/jamaoto.2018.3096>
 25. Jiam NT, Pearl MS, Carver C, Limb CJ (2016) Flat-panel CT imaging for individualized pitch mapping in cochlear implant users. *Otol Neurotol* 37(6):672–679. <https://doi.org/10.1097/MAO.0000000000001060>
 26. Rader T, Döge J, Adel Y, Weissgerber T, Baumann U (2016) Place dependent stimulation rates improve pitch perception in cochlear implantees with single-sided deafness. *Hear Res* 339:94–103. <https://doi.org/10.1016/j.heares.2016.06.013>

Publisher's Note Springer Nature remains neutral with regard to jurisdictional claims in published maps and institutional affiliations.